ATMOSPHERIC CORRECTION OF LANDSAT-8 / OLI DATA USING THE FLAASH ALGORITHM: OBTAINING INFORMATION ABOUT AGRICULTURAL CROPS.

[1]A.E.YERZHANOVA, [1]S. YE.KERIMKHULLE, [1]G.B.ABDIKERIMOVA, [2]M.MAKHANOV, [3]S.T.BEGLEROVA, [3]ZH.K.TASZHUREKOVA[3]

[1] L.N.Gumilyov Eurasian National University, Department of Information Systems, Astana, Kazakhstan
[2]L.N.Gumilyov Eurasian National University, Department of Transport, transport equipment and technologies, Nur-Sultan, Kazakhstan
[3]Non-profit limited company «Taraz Regional University named after M.KH. Dulaty», Taraz, Kazakhstan
E-mail: [1]erjanova_akbota@mail.ru, [1]kerimkhulle@gmail.com, [1]gulzira1981@mail.ru, [2]m.mahanoff@yandex.ru, [3]sbeglerova@mail.ru, [3]taszhurekova@mail.ru

ABSTRACT

The article presents studies and proposes methods for determining the objects of the underlying surface such as soil, water, soil moisture, agricultural crops and their diseases, weeds, and monitoring plant growth over vegetative periods based on the analysis of the spectral brightness coefficient of space images.
Recognition of plant species, soils, and territories from satellite images is an applied task that allows you to implement many processes in agriculture and automate the activities of farmers and large farms. These studies are aimed at creating a scientific and methodological basis for an information system in the form of a computer application on gadgets. The main tool for analyzing satellite imagery data is the clustering of data that uniquely identifies the desired objects and changes associated with various reasons.
Based on the data obtained in the course of experiments on obtaining numerical values of SLC, which are published in the press, the regularities of the behavior of the processes of reflection of vegetation, factors that impede the normal growth of plants, and the proposed clustering of the spectral ranges of wave distribution, by which the type of objects under consideration can be determined. Recognition of these causes through the analysis of the spectral brightness coefficient of satellite images will allow creating an information system for monitoring the state of plants and events to eliminate negative causes. SLC data is divided into non-overlapping ranges, i.e., they form clusters reflecting the normal development of plant species and deviations associated with negative causes. If there are deviations, then there is an algorithm that determines the cause of the deviation and proposes an action plan to eliminate the defect.
To accomplish this task, the dependence of the state of plants on the types of soils, their moisture content, the identification of weeds, the detection of diseases, and the lack of mineral and organic fertilizers were taken into account. Several negative causes associated with plant diseases require ground monitoring due to the lack of experimental data on spectral analysis of these diseases. It should be noted that the distribution of brightness spectra depends on the climatic and geographical conditions of the plant species and is unique for each region. This study refers to the Northern Kazakhstan region, where crops are grown.
In all types of space and ground monitoring of plant growth, measures are proposed to eliminate negative causes.

Keywords: *Spectral Brightness Coefficients, Earth Remote Sensing, ERS, ENVI, Landsat-8, Atmospheric Correction, FLAASH, Wavelength, Band.*

1. INTRODUCTION

In the works of scientists [12-14, 16, 18] to identify the type of the given object of the image of this object comparison with the reference image is used. For comparison, statistical methods are used for a large sample of data of two images, which require large computing resources and the use of NDVI indices has one drawback: for one NDVI - index corresponds many pairs of SBC values which entails ambiguity of the research results. For the decision of this problem, the following procedure is used: an NDVI -index image is created based on the values of the spectral brightness coefficient image, which also requires additional calculations.

In our study, we identified clusters in multispectral images, and these clusters allow for minimal computing resources. In our case, only the values of the spectral brightness coefficient and the clusters selected by us are used, which requires minimal computing resources.

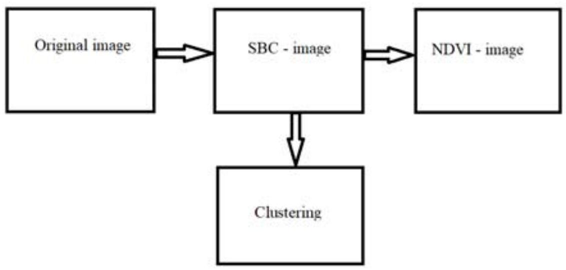

Figure 1. Image processing diagram

In many studies on this topic, data on the spectral brightness coefficient (SBC) of crops have been proposed, but they have not been analyzed from the point of clustering of crops based on satellite images.

Based on the above, the goal of our study is to cluster images of underlying surface objects using satellite images. To solve this problem, we need to solve the following tasks:

1. Analysis of existing theoretical research on the research topic;

2. Formulation of hypotheses for identifying the types of underlying surface objects such as soil, water, soil moisture, crops and their diseases, weeds, and monitoring plant growth over vegetative periods using analyses of satellite images;

3. Testing the correctness of hypotheses for crops in Northern Kazakhstan.

To decrease the volume of the article, we will consider hypotheses regarding crops and soils. All hypotheses are formulated based on image analysis

1) regarding agricultural crops for the growing season from 10.07 to 17.07 [11]:

- Hypothesis 1.1 spectral brightness coefficient of wheat is informative in the wavelength interval [800 nm; 810 nm] and belongs to the interval [79; 82];
- Hypothesis 1.2 spectral brightness coefficient of barley is informative in the wavelength interval [800 nm; 810 nm] and belongs to the interval [66; 76];
- Hypothesis 1.3 spectral brightness coefficient of oats is informative in the wavelength interval [800 nm; 810 nm] and belongs to the interval [73; 78];
- Hypothesis 1.4 spectral brightness coefficient of weeds belongs to the interval [46; min] [17].

2) soil recognition is informative in the wavelength range from 700 nm to 1300 nm [15, 19]:

- Hypothesis 1.1. If the value of the spectral brightness coefficient function belongs to the interval [6, 14], then this spectrum describes black soil
- Hypothesis 1.1. If the value of the spectral brightness coefficient function belongs to the interval [14, 24], then this spectrum describes loam
- Hypothesis 1.1. If the value of the spectral brightness coefficient function belongs to the interval [30, 44], then this spectrum describes sandy loam
- Hypothesis 1.1. If the value of the spectral brightness coefficient function belongs to the interval [60, 82], then this spectrum describes sand

In this article, to build an information system, it was necessary to select the wave ranges in which it is possible to unambiguously determine plant changes over the growing season.

The Landsat satellite allows you to measure the brightness of objects on a green (from 0.5 to 0.6 microns) area, for example, to more accurately distinguish crops, determine the area they occupy, and estimate yield. Satellites with multispectral equipment are effective in monitoring environmental pollution, searching for ocean resources, etc. [1, 26, 27].

The most common approach is the use of alternative parameters, such as linear combinations of zonal values of the spectral brightness coefficients, various spectral vegetation indices that are functions of the spectral brightness coefficient in several spectral channels, spectral features calculated based on the values of the spectral brightness coefficients, the use of transformation into principal components. In studies [11-15], various approaches are used to process multispectral space images in order to more reliably recognize different classes of vegetation.

Some scientists-researchers [16-19] proved the dependence of the spectral brightness coefficients of vegetation objects on their state.

To take into account the dynamics of the spectral brightness coefficient, it is required to obtain space images with a sufficient frequency.

ISSN: 1992-8645 www.jatit.org E-ISSN: 1817-3195

Local-scale vegetation mapping requires spatial resolution and is not available in such a sequence. Thus, the shooting frequency of the Landsat 8 satellite (spatial resolution 30 m) is once every 16 days, and most of the images are cloudy.

The OLI (Operational Land Imager) (Table 1) on Landsat-8 has been used comparatively to the ETM+ (Enhanced Thematic Mapper Plus) on Landsat-7, which has banding issues. Compared with medium- and low-resolution satellite sensors, OLI has better spatial information due to its high spatial resolution of 30 m. Besides, the OLI has a better SNR (signal-to-noise ratio) than the TM and ETM+ sensors, and there are two SWIR bands (1609 nm and 2201 nm) for atmospheric correction [2 -6, 26, 27].

Table 1. Bands of the OLI (Operational Land Imager) on Landsat-8, with band range, band center, ground sampling distance (GSD), and signal-to-noise ratio (SNR) at reference radiance [4, 5].

Band	Band Range (nm)	Band Center (nm)	GSD (m)	SNR at Reference L
Band 1 Coastal/Aerosol	433-453	443	30	232
Band 2 Blue	450-515	482	30	355
Band 3 Green	525-600	561	30	296
Band 4 Red	630-680	655	30	222
Band 5 NIR	845-885	865	30	199
Band 6 SWIR 1	1560-1660	1609	30	261
Band 7 SWIR 2	2100-2300	2201	30	326

2. PRE-PROCESSING OF SPACE IMAGES

The software complex (PC) ENVI, thanks to the programming language IDL (Interactive Data Language), is capable of providing a complex of works on processing images from multispectral and hyperspectral imaging systems. Many image analysis algorithms in the ENVI software package were specially developed for processing large amounts of information and are used in hyperspectral imagery. Most of these algorithms can also be used, albeit in a somewhat limited way, to work with multispectral imagery. The ENVI software package offers 36 vegetation indices.

3. ATMOSPHERIC CORRECTION MODULE

The peculiarity of using space images to study objects of the earth's surface is that between the elements of the earth's cover and the recording equipment there is a layer of the atmosphere and clouds. The presence of an intermediate medium causes a number of difficulties: absorption of sunlight of certain wavelengths by the atmosphere, scattering of rays, the influence of atmospheric haze, the screening effect of cloudiness, and others.

Cloudiness is the greatest interference for remote sensing data processing and object recognition. More than 50% of the earth's surface is covered with clouds at a time [29]. Some parts of our planet remain covered by clouds most of the time. Atmospheric haze reduces the contrast of displaying objects in space images, distorts the color rendering, and correct automatic processing of areas covered by atmospheric haze is impossible.

The state of the atmosphere affects the brightness values recorded by the imaging system in two ways: by scattering and absorbing energy. If the field of view is very large, then part of the scattered radiation will still be perceived by the imaging system, and in this case, the signal is amplified, and the image brightness increases.

To perform the atmospheric correction, it is necessary to know such parameters as the amount of water vapor, aerosols, visibility, etc. Direct measurement of these atmospheric parameters is rarely carried out by methods of obtaining them from spectral brightness values. The resulting coefficients are used to define highly accurate atmospheric correction models that are used to process the data. [7].

FLAASH (Fast Line-of-sight Atmospheric Analysis of Spectral Hypercubes) — is an algorithm for correcting the influence of the atmosphere based on the given models. The models used in FLAASH allow processing images obtained by any multispectral or hyperspectral imaging systems in the frequency range 400-3000 nm, including images obtained with a large deviation from the nadir [7].

The FLAASH algorithm includes the following features:

- correction of the adjacency effect that occurs due to the mixing of the brightness of neighboring pixels.

Journal of Theoretical and Applied Information Technology
15th July 2021. Vol.99. No 13

ISSN: 1992-8645 www.jatit.org E-ISSN: 1817-3195

- a tool for calculating the approximate visibility of the scene (aerosol content and the presence of haze) at frequencies equal to 660 and 2100 nm based on the methods proposed by Kaufman.

Table 2. The match-up dates of in situ measurement and OLI data acquisition over.

Location of the object under study	Cadastral number of the investigated object	Land category	OLI Image	Acquisition Date	Scene Center time
Diyev rural district, Auliekol district, Kostanay region.	12-188-039-111	Agricultural land	LC08_L1TP_160024_2018 0513_20180517	2018-05-13	06:38:02
			LC08_L1TP_160024_2018 0817_20180829	2018-08-17	06:38:27
			LC08_L1TP_160024_2018 1004_20181010	2018-10-04	06:38:46

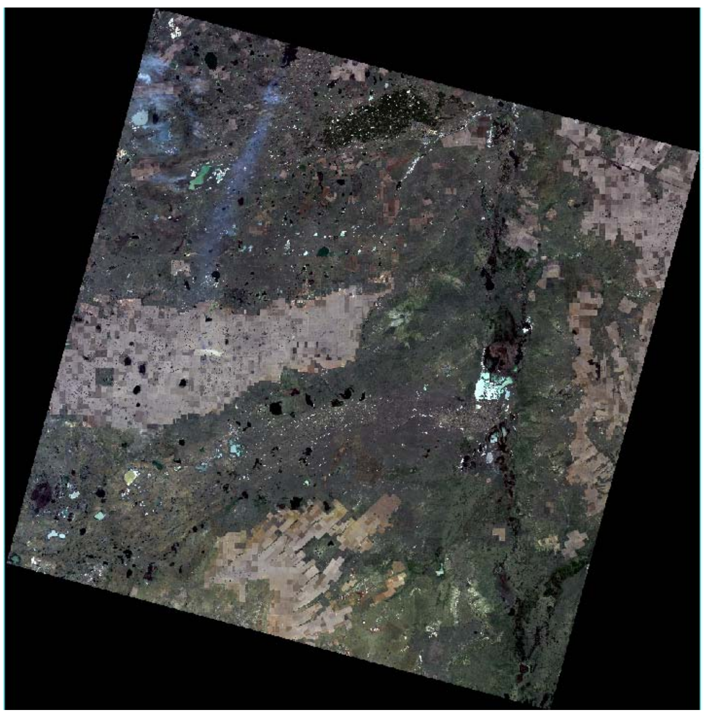

Figure 2. Source snapshot - LC08_L1TP_160024_20180513_20180517

Remote sensing has proven useful for obtaining crop information. However, obtaining reliable information from remote sensing data is challenging because the signal detected by the sensor is susceptible to atmospheric influences. The scattering and absorption of molecules and aerosols present in the atmosphere alter the net reflectivity emanating from the target. Many atmospheric correction algorithms have been developed to address these undesirable effects, however, multiple correction procedures are sensor-dependent and designed for land [8-10].

ISSN: 1992-8645 www.jatit.org E-ISSN: 1817-3195

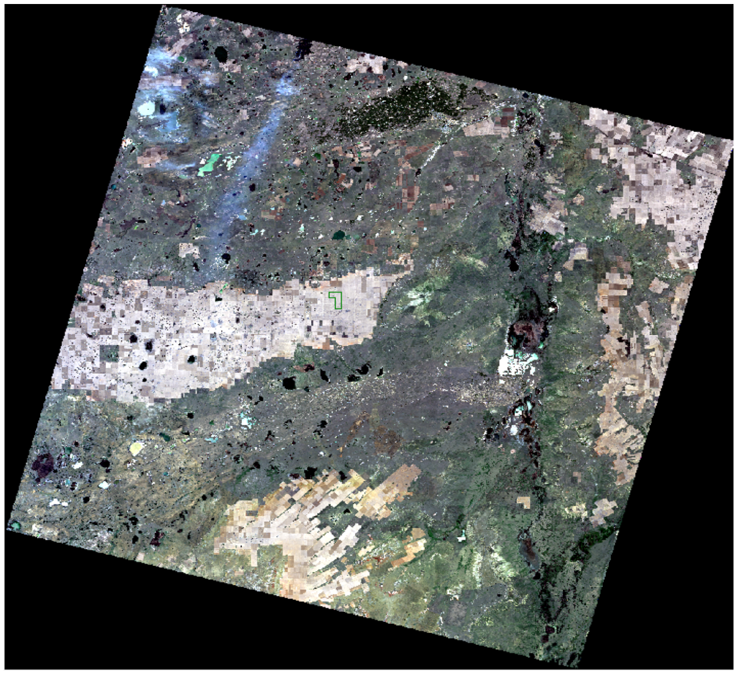

Figure 3. Snapshot after atmospheric correction - LC08_L1TP_160024_20180513_20180517

For further research, we identified the Karaganda region, Aulieata district, Diev rural district by cadastral number from a space photograph with atmospheric correction (Figure 4).

Thus, to create reliable maps of vegetation at the local level, it is necessary to develop a technique for automated decoding of vegetation cover objects based on substantiating the expediency of using multi-season data using quantitative characteristics, on determining the optimal number and moment of obtaining zonal space images.

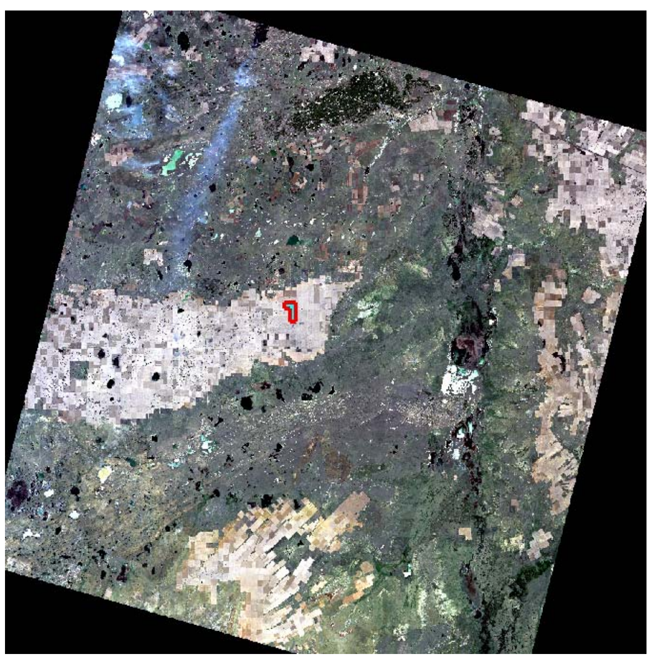

Figure 4. Allocation of the area by cadastral number 12-188-039-11

ISSN: 1992-8645 www.jatit.org E-ISSN: 1817-3195

An analysis of foreign experience [20-24] showed that the joint processing of several images obtained mainly in seasons characterizing the dynamics of the phenological development of vegetation (summer, late spring and early autumn) in different territories of the world (USA, Canada, Argentina, Egypt and others) leads to an increase in the detection accuracy of various types of land cover.

For the territory located in central Russia [25], a study was carried out in 2009 showing that the joint processing of three spring-summer images obtained from the Landsat 5 TM satellite increases the reliability of automated recognition of different types of vegetation.

The research was conducted over three months (May, August and October) (Figure 5).

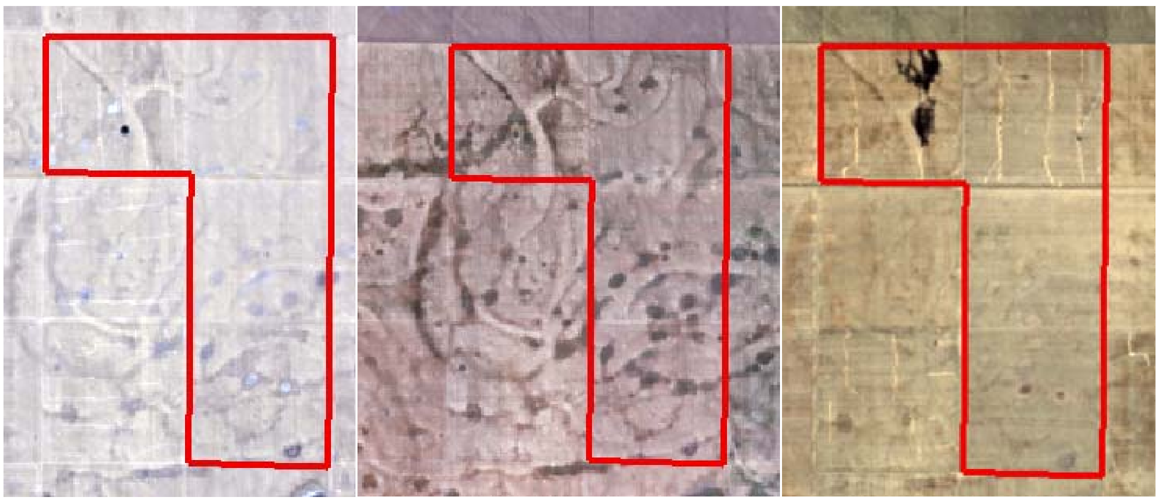

a b c

Figure 5. Highlighted areas by month (a-13.05.2018, b – 17.08.2018, c – 4.10.2018)

For images obtained from the Landsat 8 satellite, the spectral brightness coefficient is recalculated according to the formula [30]:

$$r_{\lambda} = M_{\rho} * DN + A_{\rho} \qquad (1)$$

where:

r_{λ} - is the spectral brightness coefficient;
M_{ρ} - calibration gain;
A_{ρ} - calibration offset;
DN - original numeric values.

Table 3. Standard deviation of spectral brightness coefficient for different seasons

Band	Band Center (nm)	The standard deviation of spectral brightness coefficient for different seasons StdDev×10000		
		13.05.2018	17.08.2018	4.04.2018
Band 1 Coastal/Aerosol	443	37,87	62,44	39,16
Band 2 Blue	482	40,01	72,53	43,04
Band 3 Green	561	60,27	95,79	57,66
Band 4 Red	655	76,55	149,14	69,88
Band 5 NIR	865	75,97	88,66	88,27
Band 6 SWIR 1	1609	83,46	152,92	68,58
Band 7 SWIR 2	2201	84,47	199,00	73,28

A graph (Figure 6) was constructed using the standard deviation values of the spectral brightness coefficient for each period on 7 channels (Table 3).

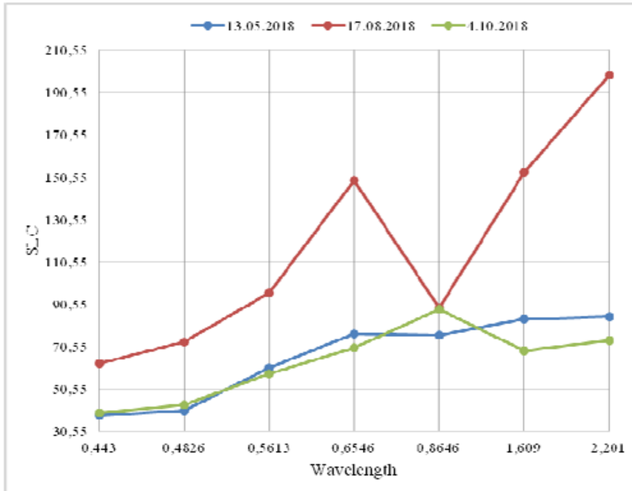

Figure 6. The Standard Deviation for the growing season

The ability to simultaneously survey in several ranges is an important advantage of remote sensing methods for studying the earth's surface, including vegetation. Each spectral channel has different information content and is suitable for solving different problems in the study of vegetation: estimating the volume of plant biomass and crop yield, determining the amount of moisture in plants and identifying plant communities prone to drought or waterlogging, vegetation affected by diseases, and others [28]

Table 4. Mean values of spectral brightness coefficient for different seasons.

Band	Band Range (nm)	Mean values of spectral brightness coefficient for different seasons		
		13.05.2018	17.08.2018	4.04.2018
Band 1 Coastal/Aerosol	443	0,09	0,07	0,05
Band 2 Blue	482	0,09	0,07	0,05
Band 3 Green	561	0,12	0,10	0,09
Band 4 Red	655	0,15	0,14	0,12
Band 5 NIR	865	0,20	0,23	0,17
Band 6 SWIR 1	1609	0,30	0,28	0,24
Band 7 SWIR 2	2201	0,27	0,22	0,19

Graph (Figure 6) was constructed using the average values of the spectral brightness coefficient for each period on 7 channels (Table 4).

The result of the FLAASH algorithm is an image with pixel values in dimensionless reflection coefficients multiplied by 10,000. Multiplication by 10,000 is performed in the course of the algorithms for converting fractional pixel values (float point) to two-byte signed integers. This procedure allows you to reduce the space occupied by the file on the hard disk, which also speeds up the process of further processing of the image. Increasing the values by 10,000 times allows you to save information in the fifth decimal place, which is more than enough for research (figure 5).

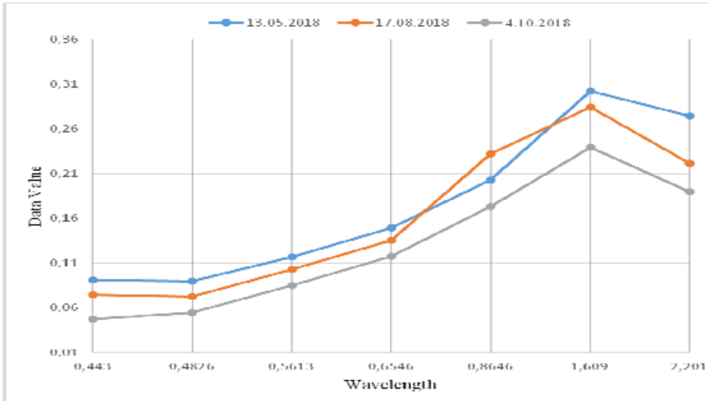

Figure 7. Average values for the growing season

The result of the FLAASH algorithm is an image with pixel values in dimensionless reflection coefficients multiplied by 10,000. Multiplication by 10,000 is performed in the course of the algorithms for converting fractional pixel values (float point) to two-byte signed integers. This procedure allows you to reduce the space occupied by the file on the hard disk, which also speeds up the process of further processing of the image. Increasing the values by 10,000 times allows you to save information in the fifth decimal place, which is more than enough for research (figure 5).

4. CONCLUSION

A plot of agricultural land in the Kostanay region, Auliekol district, Dievsky s/o, cadastral number 12-188-039-111, according to the growing seasons 05/13/2018, 08/17/2018, 10/10/2018 (table 1) was considered. The work was performed in the ENVI 5.3 environment.- Remote sensing data include information not only about the surface but also about the state of the atmosphere. Based on the given models, the FLAASH algorithm was carried out using the original images. (figure 2)

- According to the cadastral number, one object with an area of 272.08 square meters was allocated for different growing seasons. km (Figure 4). Spectral values were plotted for 7 channels using standard deviations and mean values of the created object for each growing season.

- Comparing the values obtained in Tables 3 and 4 for the selected area, the values of 17.08.2018 differ from the remaining two months, as in August it is possible to determine the types of crops. Since the field is now sown in May, the growth on the ground looks the same, it is impossible to determine. And in October, when the crops are harvested, only the black earth is visible. In particular, from Tables 3 and 4 we can classify the types of cereals with the data for August.

- Based on the results of this work, we can recognize the types of crops and monitor the growth of crops by vegetative periods (Figure 6, 7).

REFRENCES:

[1] Kashkin, VB Remote sensing of the earth from space. Digital image processing [text]: textbook. Benefit. / V. B. Kashkin, A. I. Sukhinin. - M .: Logos, 2001 .- P 264.

[2] Knight, E.; Kvaran, G. Landsat-8 Operational Land Imager Design, Characterization and Performance. Remote Sens. 2014, 6, 10286–10305.

[3] Concha, J.A.; Schott, J.R. Retrieval of color-producing agents in Case 2 glasses of water using Landsat 8. Remote Sens. Environ. 2016, 185, 95–107.

[4] Irons, J.R.; Dwyer, J.L.; Barsi, J.A. The next Landsat satellite: The Landsat Data Continuity Mission. Remote Sens. Environ. 2012, 122, 11–21.

[5] Wang D., Ma R., Xue K., Loiselle S.A. The Assessment of Landsat-8 OLI Atmospheric Correction Algorithms for Inland Waters // Remote Sensing. 2019, No 11 (2), 169. https://doi.org/10.3390/rs11020169.

[6] Wang D., Ma R., Xue K., Li J. Improved atmospheric correction algorithm for Landsat 8–OLI data in turbid waters: a case study for the Lake Taihu, China // Vol. 27, Issue 20, pp. 1400-A1418. (2019). https://doi.org/10.1364/OE.27.0A1400.

ISSN: 1992-8645 www.jatit.org E-ISSN: 1817-3195

[7] Kolesnikova O., Cherepanov A. New ENVI software opportunities for processing multispectral and hyperspectral data // Geomatics. 2009. No. 3. P. 24-27.
[8] Conel, J.E., Green, R.O., Vane, G., Bruegge, C.J., & Alley, R. E.(1987).AIS-2radiometryandacomparisonofmethods for the recovery of ground reflectance. In G. Vane (Ed.), Proceedings of the 3rd Airborne Imaging Spectrometer Data Analysis Workshop JPL Publ (Vols. 87–30, pp. 18 −47). Pasadena, CA: Jet Propulsion Laboratory.
[9] Kruse, F.A. (1988). Use of airborne imaging spectrometer data to map minerals associated with hydrothermally altered rocks in the northern Grapevine Mountains, Nevada, and California. Remote Sensing of Environment, 24, 31 – 51.
[10] L. De Keukelaere, S. Sterckx, S. Adriaensen, E. Knaeps, I. Reusen, C. Giardino, M. Bresciani, P. Hunter, C. Neil, D. Van der Zande & D. Vaiciute (2018) Atmospheric correction of Landsat-8/OLI and Sentinel-2/MSI data using iCOR algorithm: validation for coastal and inland waters, European Journal of Remote Sensing, 51:1, 525-542, DOI: 10.1080/22797254.2018.1457937.
[11] Terekhin E.A. Analysis of satellite data channels Landsat TM for assessing the characteristics of forest plantations of the Forest-steppe province of the Central Russian Upland // Earth Research from Space. 2012. No. 2 P. 53-61.
[12] Terekhin E.A. Informativeness of spectral vegetation indices for decoding agricultural vegetation // Modern problems of remote sensing of the Earth from space. 2012 T. 9.No.4. P. 243-248
[13] Terekhin E.A. A method for mapping long-term changes in forests based on an analysis of their spectral characteristics from a series of satellite data at different times. Investigation of the Earth from Space, 2013, no. 5, p. 62-69
[14] Borisova M.V. Development of a technique for automated decoding of a space image of the earth's surface using a system of n-dimensional spectral features: dissertation for the degree of candidate of technical sciences. 25.00.34. Moscow, 2010 – p. 185.
[15] Zhirin V.M., Knyazeva S.V. Evaluation of the possibilities of decoding forest-forming species from IKONOS satellite images / Modern problems of remote sensing of the Earth from space. 2009. B.6. T.2. p. 373-379.
[16] Krinov, E.L. Spectral reflectivity of natural formations // E.L. Krinov; USSR Academy of Sciences, Lab. aerial methods. - M .; L .: Publishing House of the Academy of Sciences of the USSR, 1947. - 270, [2] p. - Bibliography: p. 114-116.
[17] Malinnikov V.A. Theory and methods of information support for land monitoring (thematic processing of video images): dissertation for the degree of Doctor of Technical Sciences. 05.24.04. Moscow, 1999 - 317 p.
[18] Malinnikov V.A., Stetsenko A.F., Altynov A.E., Popov S.M. Monitoring of the natural environment by aerospace means. Textbook for university students. - M .: Ed. MIIGAiK. 2008, 145 p.
[19] Malinnikov V.A., Stetsenko A.F., Altynov A.E., Popov S.M. Aerolandscape spectrometry. Textbook for students M .: Izd. MIIGAiK. UPP "Reprographia", 2008, 120 p.
[20] Kalensky Z.D., Moore W.C., Campbell G.A., D.A. Wilson, Scott A.J. Summary forest resource data from Landsat images. Environment Canada, Canadian Forestry Service, 1981, Petawawa National Forestry Institute, Chalk River, Ontario.
[21] Lo T. H. C., Scarpace F. L., Lillesand T. M. Use of multitemporal spectral profiles in agricultural land-cover classification // Photogrammetric Engineering and Remote Sensing, 1986, 52, 535-544.
[22] Pax-Lenney M., Woodcock C. E. Monitoring agricultural lands in Egypt with multitemporal Landsat TM imagery: how many images are needed? // Remote Sensing of Environment, 59, 1997. pp. 522-529.
[23] Oetter D. R., Cohen W. B., Berterretche M., Maiersperger T. K., Kennedy R. E. Land cover mapping in an agricultural setting using multiseasonal Thematic Mapper data. Remote Sensing of Environment, 76, 2001, P. 139–155.
[24] Guerschman J. P., Paruelo J. M., Bella C. D., Giallorenz M. C., Pacin F. Land cover classification in the Argentine Pampas

ISSN: 1992-8645 www.jatit.org E-ISSN: 1817-3195

using multi-temporal Landsat TM data // International Journal of Remote Sensing, 24, 2003, P. 3381–3402.

[25] Marchukov V.S., Stytsenko E.A. Deciphering the vegetation cover using spectral-temporal features // Research of the Earth from Space. 2012, no. 1, p. 77-88.

[26] Landsat 8 [Electronic resource]. - Access mode https://landsat.gsfc.nasa.gov/landsat-data-continuity-mission/, free access (date of access 03/11/2017).

[27] Landsat history. [Electronic resource]. - Access mode http://landsat.gsfc.nasa.gov/about/history/, free access (date of appeal 11.03.2017).

[28] Stytsenko E.A. Development of a technique for automated decoding of vegetation cover with the integrated use of multi-season zonal space images. // Moscow. 2018.S. 213.

[29] Bartalev S.A., Egorov V.A., Lupyan E.A., Plotnikov D.E., Uvarov I.A. Recognition of arable lands based on long-term satellite data of the MODIS spectroradiometer and locally adaptive classification // Computer Optics. 2011.Vol. 35.No. 1.P. 103-116.

[30] Using the USGS Landsat 8 Product [Electronic resource]. - Access mode https://landsat.usgs.gov/using-usgs-landsat-8-product, free access (date of access 03/11/2017).